JOURNAL OF SOLID STATE CHEMISTRY 115, 373–378 (1995)

# $K_3Nb_5GeO_{16} \cdot 2H_2O$, a New Hydrated Potassium Niobium Germanate Containing a Two-Dimensional Channel Network

William T. A. Harrison,*,[1] Thurman E. Gier,† and Galen D. Stucky†

*Department of Chemistry, University of Houston, Houston, Texas 77204-5641; and †Department of Chemistry, University of California, Santa Barbara, California 93106-9510

Received January 28, 1994; in revised form August 12, 1994; accepted August 17, 1994

We report the high-pressure/high-temperature hydrothermal synthesis and single crystal structure of $K_3Nb_5GeO_{16} \cdot 2H_2O$, a new hydrated potassium niobium germanate. $K_3Nb_5GeO_{16} \cdot 2H_2O$ consists of a three-dimensional network of edge- and corner-sharing $NbO_6$ and $GeO_4$ groups, enclosing large, intersecting channels in the [001] and [010] directions, where the guest cations and water molecules are located. $K_3Nb_5GeO_{16} \cdot 2H_2O$ is briefly compared with other known alkali-metal niobium germanates and related phases. Crystal data: $K_3Nb_5GeO_{16} \cdot 2H_2O$, $M_r = 946.44$, orthorhombic, space group *Pmma* (No. 51), $a = 7.5265(8)$ Å, $b = 10.4258(9)$ Å, $c = 10.7692(9)$ Å, $V = 845$ Å$^3$, $Z = 2$, $R(F) = 5.69\%$, and $R_w(F) = 5.59\%$ [1350 observed reflections with $I > 3\sigma(I)$]. 

## INTRODUCTION

The structures of several alkali-metal niobium germanates have been described over the past few years. $RbNb(GeO_3)_3$ (1) consists of a vertex-sharing (Nb–O–Ge, Ge–O–Ge bonds), three-dimensional network of $NbO_6$ and triangular $(GeO_3)_3$ units, enclosing one-dimensional channels occupied by rubidium cations. The framework of $K_{10}Nb_{22}Ge_4O_{68}$ (2) is built up from a very complex network of corner-sharing (via Nb–O–Nb, Nb–O–Ge, and Ge–O–Ge) distorted $NbO_6$ and $Ge_2O_7$ units, while that of $K_6Nb_6Ge_4O_{26}$ (3), also built up from $NbO_6$ and $Ge_2O_7$ groups, forms one-dimensional "tungsten bronze"-like pentagonal channels occupied by the guest $K^+$ species. $NaNbOGeO_4$ (4), which is isostructural with the mineral sphene ($CaTiOSiO_4$) (5), consists of infinite chains of corner-sharing $NbO_6$ octahedra crosslinked by $GeO_4$ groups which enclose the sodium cations. $LiNbOGeO_4$ (6) contains $NbO_6$ and $GeO_4$ units, linked via Nb–O–Nb and Nb–O–Ge bonds, and enclosing the $Li^+$ cations, but in a different arrangement to that found in $NaNbOGeO_4$. $Li_{17}GeNb_{18}O_{47}$ (7) is the product of lithium insertion into Wadsley–Roth-type phases. In addition to these *M*Nb/Ge/O phases, numerous *M*W/P/O and *M*Mo/P/O phases have been characterized over the past few years (8–11) which show similar variety in their structures and complex polyhedral connectivities.

Although all these materials are built up from the same basic $NbO_6$ and $GeO_4$ units, they show considerable variety in their polyhedral connectivity. Linkages involving Nb–O–Nb, Nb–O–Ge, and Ge–O–Ge bonds are all possible, and the particular alkali-metal cation appears to have a significant effect in "structure directing" to a particular anionic Nb/Ge/O framework configuration.

In this paper we report one result of our exploratory hydrothermal syntheses in the $K/Nb/Ge/O/H_2O$ system. $K_3Nb_5GeO_{16} \cdot 2H_2O$ is a new structure containing a three-dimensional network of $NbO_6$ and $GeO_4$ units, linked via Nb–O–Ge and Nb–O–Nb vertices, and Nb–(O,O')–Nb edges, and represents the first well-characterized hydrated *M*/Nb/Ge/O material. The $K_3Nb_5GeO_{16} \cdot 2H_2O$ framework encloses a two-dimensional network of large channels, occupied by disordered potassium cations and water molecules.

## SYNTHESIS AND INITIAL CHARACTERIZATION

$K_3Nb_5GeO_{16} \cdot 2H_2O$ was prepared as follows: 0.157 g $GeO_2$ (1.5 mmole), 0.133 g $Nb_2O_5$ (0.5 mmole), 0.183 g KOH (0.75 mmole), and 0.3 ml $H_2O$ were sealed in a gold tube, and placed in a Leco Tem-Pres hydrothermal bomb. The tube was heated to 750°C for 46 hr, and then slowly cooled from 750 to 550°C over a 20-hr period. The estimated maximum pressure attained was 30,000 psi. Upon cooling to ambient temperature, the tube was broken open, and a number of plate-like (maximum dimensions ~2 × 0.22 × 0.2 mm) transparent crystals were recovered by vacuum filtration. Other crystal morphologies were also present, and these are being investigated further. All these crystals are air-stable. A powder second-harmonic-generation (PSHG) test (12) on selected, ground $K_3Nb_5GeO_{16} \cdot 2H_2O$ crystals gave a null response, indicating that $K_3Nb_5GeO_{16} \cdot 2H_2O$ probably

[1] To whom correspondence should be addressed.



0022-4596/95 $6.00

crystallizes in a centrosymmetric space group. An X-ray powder pattern of $K_3Nb_5GeO_{16} \cdot 2H_2O$ could successfully be simulated using the single crystal parameters derived below.

## CRYSTAL STRUCTURE DETERMINATION

The structure of $K_3Nb_5GeO_{16} \cdot 2H_2O$ was determined by single-crystal X-ray methods. After many twinned (double/multiple $\omega$-scans) crystals were examined and rejected, an untwinned, transparent wedge (dimensions $\sim 0.8 \times 0.4 \times 0.1$–$0.02$ mm) was broken from a larger plate, and found to be suitable for data collection. Preliminary $\omega$-scans indicated instrumental resolution peak widths (scan-width = 0.15°–0.17°).

Room temperature [25(2)°C] intensity data were collected on a Huber automated 4-circle diffractometer (graphite-monochromated Mo$K\alpha$ radiation, $\lambda = 0.71073$ Å). After locating and centering 25 reflections, unit cell constants were optimized by least-squares refinement, resulting in orthorhombic lattice parameters of $a = 10.4258(9)$ Å, $b = 10.7692(9)$ Å, and $c = 7.5265(8)$ Å (esd's in parentheses). Intensity data were collected in the $\theta$-$2\theta$ scanning mode with standard reflections monitored for intensity changes throughout the data collection (negligible variation observed). The scan speed was 6°/min with a scan range of 1.3° below $K\alpha_1$ to 1.6° above $K\alpha_2$. The raw data were reduced to $F$ and $\sigma(F)$ values by using a Lehmann–Larsen profile-fitting routine (13) and the normal corrections for Lorentz and polarization effects were made. The systematic absence condition in the reduced data ($h0l$, $l \neq 2n$) was consistent with space groups $Pmc2_1$, $P2cm$, and $Pmcm$ (1929 data input, 106 reflections systematically absent or with $I_{obs} \leq 0$, 1350 reflections with $I > 3\sigma(I)$ after merging [$R_{Int} = 3.76\%$]).

The initial model of the crystal structure was developed in space group $Pmc2_1$, with heavy-atom positions (Nb, Ge) located using the direct-methods program SHELXS-86 (14). Other atom positions were located from iterated Fourier difference maps during the refinement. High correlations and instabilities were apparent, indicating additional symmetry, which could be accounted for in space group $Pmcm$ (nonstandard setting of $Pmma$, No. 51). The data were transformed to accord with the standard setting of this space group, such that $a' = 7.5265(8)$ Å, $b' = 10.4258(9)$ Å, and $c' = 10.7692(9)$ Å. $Pmma$ was then assumed for the remainder of the crystallographic analysis: This centrosymmetric space group is consistent with the null PSHG signal observed for $K_3Nb_5GeO_{16} \cdot 2H_2O$. Several extra-framework guest species were located in sites which required partial occupancy, because of unreasonably close guest–guest distances. These guest sites were assigned to potassium cations or oxygen atoms (water molecules) on the basis of distance/angle and charge-balancing criteria, as noted below. Attempts to refine the anisotropic thermal parameters of the guest species led to unstable refinements and high correlations.

After isotropic refinement, an empirical absorption correction (DIFABS) (15) was applied, but this had little effect on Nb/Ge/O atom anisotropic thermal factors or residuals, and later refinements reverted to the "raw," as-measured $F_o$ values. The final cycles of full-matrix least-squares refinement minimized the function $\Sigma w_i(F_o - F_c)^2$ (Tukey–Prince weighting scheme (16)), and included anisotropic temperature factors for Nb, Ge, and "framework" O atoms, and a secondary extinction correction (17), which helped to correct for a $F_o < F_c$ trend seen in strong, low-angle reflections. Complex, neutral-atom scattering factors were obtained from the "International Tables" (18). At the end of the refinement, analysis of the various trends in $F_o$ versus $F_c$ revealed no unusual effects. The least-squares, Fourier, and subsidiary calculations were performed using the Oxford CRYSTALS system (19), running on a DEC MicroVAX 3100 computer. Supplementary tables of observed and calculated structure factors and anisotropic thermal factors are available from the authors. Crystallographic and data-collection data for $K_3Nb_5GeO_{16} \cdot 2H_2O$ are summarized in Table 1.

A unit-cell stoichiometry of $K_{6.12(5)}Nb_{10}Ge_2O_{32} \cdot 3.96(6)$

TABLE 1
**Crystallographic Parameters for $K_3Nb_5GeO_{16} \cdot 2H_2O$**

| | |
|---|---|
| Empirical formula | $Nb_5Ge_1K_3O_{18}H_4$ |
| Formula wt. | 946.44 |
| Habit | Colorless wedge |
| Crystal system | Orthorhombic |
| $a$ (Å) | 7.5265(8) |
| $b$ (Å) | 10.4258(9) |
| $c$ (Å) | 10.7692(9) |
| $V$ (Å$^3$) | 845.06 |
| $Z$ | 2 |
| Space group | $Pmma$ (No. 51) |
| $T$ (°C) | 25(1) |
| $\lambda$(Mo$K\alpha$) (Å) | 0.71073 |
| $\rho_{calc}$ (g/cm$^3$) | 3.719 |
| $\mu$(Mo$K\alpha$) (cm$^{-1}$) | 56.99 |
| Absorption correction | None |
| $hkl$ limits | $0 \rightarrow 11$, $0 \rightarrow 15$, $0 \rightarrow 16$ |
| Total data | 1929 |
| Observed data[a] | 1350 |
| Parameters refined | 86 |
| $R(F)$[b] (%) | 5.69 |
| $R_w(F)$[c] (%) | 5.59 |

[a] $I > 3\sigma(I)$ after merging.
[b] $R = 100 \times \Sigma \|\|F_o\| - \|F_c\|\|/\Sigma|F_o|$.
[c] $R_w = 100 \times [\Sigma w(|F_o| - |F_c|)^2/\Sigma w|F_o|^2]^{1/2}$, with $w_i$ as described in the text.

TABLE 2
*Atomic Positional/Thermal Parameters for* $K_3Nb_5GeO_{16} \cdot 2H_2O$

| Atom | $W^a$ | $x$ | $y$ | $z$ | $U^b_{eq}$ | Occupancy[c] |
|---|---|---|---|---|---|---|
| K(1) | 4*g* | 0 | 0.1307(8) | 0 | 0.042(2)[d] | 0.47(2) |
| K(21) | 4*k* | 1/4 | 0.3242(7) | 0.2473(5) | 0.013(2)[d] | 0.49(2) |
| K(22) | 4*k* | 1/4 | 0.2799(8) | 0.2220(6) | 0.020(2)[d] | 0.45(2) |
| K(3) | 2*d* | 0 | 1/2 | 1/2 | 0.030(5)[d] | 0.27(2) |
| Nb(1) | 4*k* | 1/4 | 0.3265(1) | −0.24087(9) | 0.0111 | |
| Nb(2) | 2*b* | 0 | 1/2 | 0 | 0.0161 | |
| Nb(3) | 4*h* | 0 | −0.16506(9) | 1/2 | 0.0127 | |
| Ge(1) | 2*e* | 1/4 | 0 | −0.2857(1) | 0.0082 | |
| O(1) | 2*f* | 1/4 | 1/2 | 0.0599(9) | 0.0043 | |
| O(2) | 8*l* | −0.0651(7) | −0.3661(5) | 0.1237(4) | 0.0084 | |
| O(3) | 4*j* | −0.061(1) | 0 | 0.3854(6) | 0.0091 | |
| O(4) | 4*k* | 1/4 | 0.1367(7) | −0.1933(7) | 0.0124 | |
| O(5) | 8*l* | −0.0654(7) | −0.2754(5) | 0.3713(4) | 0.0099 | |
| O(6) | 2*f* | 1/4 | 1/2 | −0.3061(9) | 0.0086 | |
| O(7) | 4*k* | 1/4 | 0.1499(7) | 0.4424(6) | 0.0105 | |
| O(10) | 4*j* | 0.827(4) | 1/2 | 0.584(3) | 0.053(9)[d] | 0.49(4) |
| O(11) | 4*k* | 1/4 | 0.067(3) | 0.184(3) | 0.049(9)[d] | 0.50(4) |

[a] Wyckoff letter.
[b] $U_{eq}$ (Å$^2$) = $(U_1U_2U_3)^{1/3}$.
[c] Fractional site occupancy, if not unity.
[d] $U_{iso}$ (Å$^2$).

$H_2O$ resulted from the X-ray refinement, and the formula is therefore written as $K_3Nb_5GeO_{16} \cdot 2H_2O$ ($Z = 2$).

## RESULTS

Final atomic positional and thermal parameters for $K_3Nb_5GeO_{16} \cdot 2H_2O$ are listed in Table 2, and selected geometrical data are provided in Tables 3 and 4. The asymmetric unit of the three-dimensional framework structure of $K_3Nb_5GeO_{16} \cdot 2H_2O$ consists of three octahedrally coordinated niobium atoms, one tetrahedral germanium atom, and seven oxygen atoms, in various coordinations, as described below. The "guest" species consist of four distinct, partially occupied potassium cations, and two partially occupied water-molecule oxygen

TABLE 3
**Bond Distances (Å) for** $K_3Nb_5GeO_{16} \cdot 2H_2O$[a]

| | | | |
|---|---|---|---|
| K(1)–O(2) × 2 | 2.835(9) | K(1)–O(4) × 2 | 2.807(5) |
| K(1)–O(11) × 2 | 2.81(2) | | |
| K(21)–O(1) | 2.727(9) | K(21)–O(2) × 2 | 2.755(6) |
| K(21)–O(5) × 2 | 2.771(6) | K(21)–O(7) | 2.778(8) |
| K(21)–O(10) × 2 | 2.65(2) | K(21)–O(11) | 2.77(3) |
| K(22)–O(1) | 2.883(9) | K(22)–O(2) × 2 | 2.748(6) |
| K(22)–O(5) × 2 | 2.868(6) | K(22)–O(7) | 2.734(9) |
| K(22)–O(10) × 2 | 3.16(2) | | |
| K(3)–O(10) × 2 | 2.62(3) | K(3)–O(5) × 2 | 2.766(5) |
| K(3)–O(6) × 2 | 2.811(7) | | |
| Nb(1)–O(2) × 2 | 1.923(5) | Nb(1)–O(4) | 2.045(8) |
| Nb(1)–O(5) × 2 | 2.046(5) | Nb(1)–O(6) | 1.940(3) |
| Nb(2)–O(1) × 2 | 1.989(3) | Nb(2)–O(2) × 4 | 1.991(5) |
| Nb(3)–O(3) × 2 | 2.167(4) | Nb(3)–O(5) × 2 | 1.867(5) |
| Nb(3)–O(7) × 2 | 1.987(2) | | |
| Ge(1)–O(3) × 2 | 1.782(7) | Ge(1)–O(4) × 2 | 1.738(8) |
| O(10)–O(5) × 2 | 2.99(2) | O(10)–O(6) | 3.04(3) |
| O(10)–O(10) | 3.17(6) | O(11)–O(3) × 2 | 3.27(2) |
| O(11)–O(7) | 2.92(3) | | |

[a] Apparent short contacts due to disorder of the guest atoms have been excluded.

TABLE 4
**Selected Bond Angles(°) for** $K_3Nb_5GeO_{16} \cdot 2H_2O$

| | | | |
|---|---|---|---|
| O(2)–Nb(1)–O(2) | 92.7(3) | O(2)–Nb(1)–O(4) | 92.5(2) |
| O(2)–Nb(1)–O(5) | 90.9(2) | O(2)–Nb(1)–O(5) | 175.9(2) |
| O(4)–Nb(1)–O(5) | 85.4(2) | O(5)–Nb(1)–O(5) | 85.5(3) |
| O(2)–Nb(1)–O(6) | 92.2(2) | O(4)–Nb(1)–O(6) | 173.3(3) |
| O(5)–Nb(1)–O(6) | 89.7(2) | | |
| O(1)–Nb(2)–O(1) | 180[a] | O(1)–Nb(2)–O(2) | 90.9(2) |
| O(1)–Nb(2)–O(2) | 89.1(2) | O(2)–Nb(2)–O(2) | 180[a] |
| O(3)–Nb(3)–O(3) | 74.8(3) | O(3)–Nb(3)–O(5) | 90.6(2) |
| O(3)–Nb(3)–O(5) | 165.4(2) | O(5)–Nb(3)–O(5) | 104.0(3) |
| O(3)–Nb(3)–O(7) | 85.0(3) | O(3)–Nb(3)–O(7) | 87.7(3) |
| O(5)–Nb(3)–O(7) | 91.8(3) | O(5)–Nb(3)–O(7) | 93.9(3) |
| O(7)–Nb(3)–O(7) | 170.9(4) | | |
| O(3)–Ge(1)–O(3) | 105.9(4) | O(3)–Ge(1)–O(4) | 110.2(2) |
| O(4)–Ge(1)–O(4) | 110.1(5) | | |
| Nb(2)–O(1)–Nb(2) | 142.2(5) | Nb(1)–O(2)–Nb(2) | 140.1(3) |
| Nb(3)–O(3)–Nb(3) | 105.2(3) | Nb(3)–O(3)–Ge(1) | 120.8(2) |
| Nb(1)–O(4)–Ge(1) | 130.5(4) | Nb(1)–O(5)–Nb(3) | 148.1(3) |
| Nb(1)–O(6)–Nb(1) | 137.6(5) | Nb(3)–O(7)–Nb(3) | 142.4(4) |

[a] By symmetry.

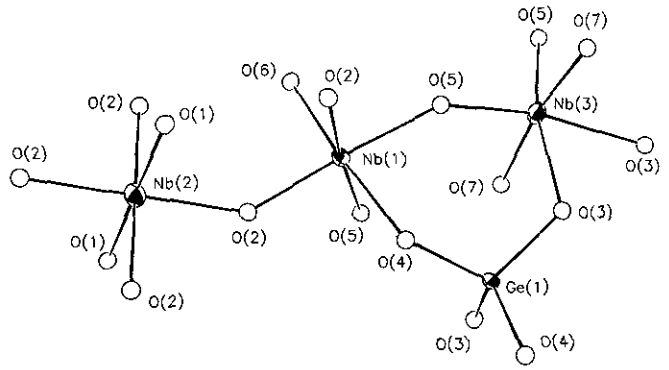


FIG. 1. ORTEP view of the Nb/Ge/O asymmetric unit in $K_3Nb_5GeO_{16} \cdot 2H_2O$, showing the atom labeling scheme (50% thermal ellipses).

atoms. No protons could be found from Fourier difference maps, nor could they be unambiguously located on the basis of geometrical criteria. The "framework" asymmetric unit and atom-labeling scheme of $K_3Nb_5GeO_{16} \cdot 2H_2O$ is shown in Fig. 1, and a unit-cell view down [100] is shown in Fig. 2.

The main structural motif in $K_3Nb_5GeO_{16} \cdot 2H_2O$ consists of infinite double columns of $Nb(3)O_6$ octahedra which propagate via O(7) vertices in the [100]-direction. These octahedral pairs then share edges [via 2 × O(3)] in the **b**-direction. The site symmetry of Nb(3) is (.2.), and the average Nb–O bond distance of 2.007(2) Å is in accordance with that expected from the ionic-radii sum of $Nb^{5+}$ and $O^{2-}$ of 2.00 Å (20). Also propagating in the **a**-direction are single, vertex-sharing columns of $Nb(2)O_6$ octahedra (Nb site symmetry = .2/*m*.), linked to each other via O(1) [$d_{av}$(Nb(2)–O) = 1.990(2) Å]. The third niobium atom [Nb(1), site symmetry = *m*..] partakes in one-dimensional $[NbO_6–NbO_6–GeO_4]_n$ strings which are oriented in the **b**-direction, with $d_{av}$(Nb–O) = 1.987(3) Å. These Nb(1)/Ge/O strings crosslink the double and single octahedral Nb/O columns into a three-dimensional network: the Nb(1)–O–Nb(1) link is provided by O(6), and the Nb(1)–O–Ge(1) link by O(4). The Ge atom shows typical tetrahedral coordination [$d_{av}$(Ge–O) = 1.760(4) Å; ionic radii sum for $Ge^{4+}$ and $O^{2-}$ = 1.75 Å; Ge site symmetry = *mm*2], and the $GeO_4$ tetrahedron links adjacent Nb(1) units via O(4) as noted above. Its other vertices [2 × O(3)] provide the links to the $Nb(3)O_6$ double columns. Brese–O'Keefe bond valence sum (BVS) calculations (21) for the Nb and Ge atoms are in good accord with the values expected (Nb = 5.00, Ge = 4.00) for these species: BVS[Nb(1)] = 4.95; BVS[Nb(2)] = 4.84; BVS[Nb(3)] = 4.88; BVS[Ge(1)] = 3.88. The $Nb(3)O_6$ octahedron is somewhat distorted, whereas the Nb(1) and Nb(2) centered units are close to regular octahedral geometry.

Of the seven framework oxygen atoms, five [O(1), O(2), O(5), O(6), O(7)] form Nb–O–Nb bridges, with $\theta_{av}$ = 142.1° (SD of mean = 3.9°). O(4) makes a Nb–O–Ge connection, and O(3) is bonded to two niobium atoms and one germanium species (Table 3).

The extra-framework species are situated in the following coordination environments: K(1) (Fig. 3) occupies a distorted trigonal prismatic geometry, in the large 8-ring [100] channel, and has $d_{av}$(K–O) = 2.817(6) Å, BVS = 0.94. K(21) (Fig. 4) and K(22) (Fig. 5) are both irregularly

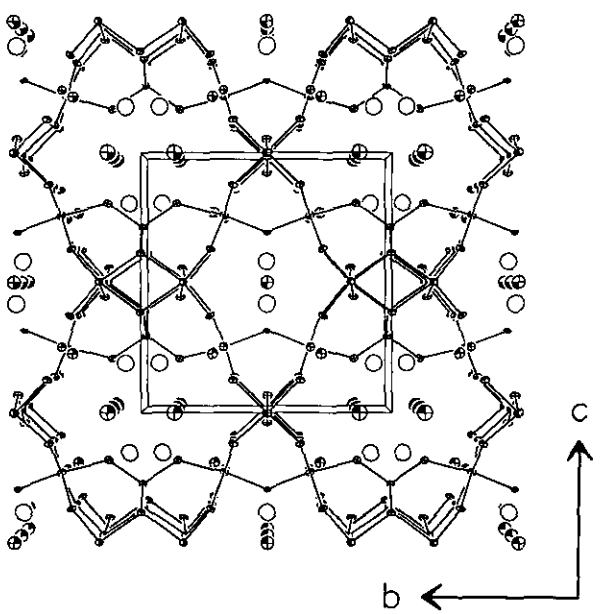


FIG. 2. ORTEP view of the $K_3Nb_5GeO_{16} \cdot 2H_2O$ structure (50% thermal ellipses), viewed down [100]. The extra-framework $K^+$ ions (shaded circles) and water molecules (plain circles) are discussed in the text.

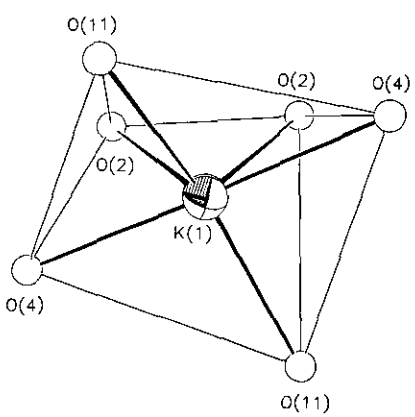


FIG. 3. ORTEP view of the K(1) coordination environment in $K_3Nb_5GeO_{16} \cdot 2H_2O$, with K represented by a shaded sphere, and O atoms by spheres of arbitrary radius. Nonbonding O · · · O contacts < 4.6 Å are represented by thin lines.

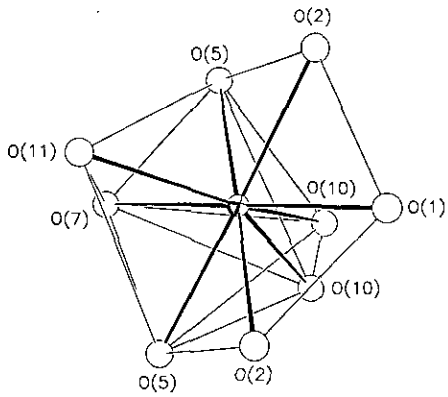


FIG. 4. ORTEP view of the K(21) coordination environment in $K_3Nb_5GeO_{16} \cdot 2H_2O$, with K represented by a shaded sphere, and O atoms by spheres of arbitrary radius. Nonbonding O · · · O contacts < 3.8 Å are represented by thin lines.

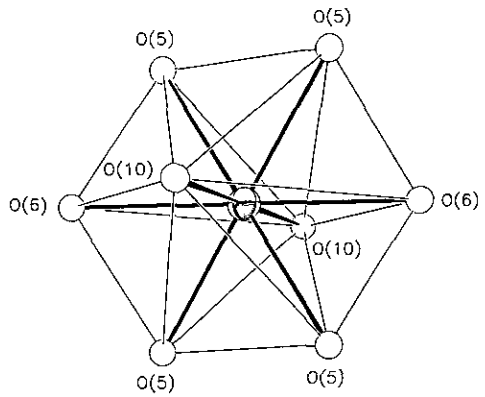


FIG. 6. ORTEP view of the K(3) coordination environment in $K_3Nb_5GeO_{16} \cdot 2H_2O$, with K represented by a shaded sphere, and O atoms by spheres of arbitrary radius. Nonbonding O · · · O contacts < 4.6 Å are represented by thin lines.

ninefold coordinated by oxygen atoms, and their coordinations are virtual "mirror images." A $d_{av}$(K–O) of 2.747(5) Å, and allowing for disorder, a BVS of 1.51 result for K(21), with comparable values of $d_{av}$(K–O) = 2.858(4) Å, and BVS = 1.04 for K(22). This BVS value for K(21) is high compared to the expected value of 1.00 for potassium, but the partial occupancy effects of the disordered guest water molecules which are bound to K(21) with short K–O distances [2.65(2) Å for O(10), 2.77(3) Å for O(11)] complicate the situation. We also note that K(21) and K(22) are separated by only ~0.54 Å, and represent a "split," fully occupied, K(2) site located at $\frac{1}{4}$, ~0.302, ~0.234: The fractional site occupancies of the K(21) and K(22) sites (Table 2) sum to unity, within experimental error. The isotropic thermal factors of these "split" positions are somewhat smaller than the $U_{iso}$ values for K(1) and K(3). Thus, the K(21) and K(22) sites could also be modeled by a single K atom at ($\frac{1}{4}$, ~0.302, ~0.234) with highly anisotropic thermal motion in the [010] channel direction, which would lack the short K–$OH_2$ bonds noted above. K(3), which occupies the smaller 6-ring [100] channel (*vide infra*) is eightfold coordinated by O atoms, in very distorted square antiprismatic geometry. [Fig. 6, $d_{av}$(K(3)–O) = 2.732(8) Å, BVS[K(3)] = 1.21]. The extra-framework water mole-

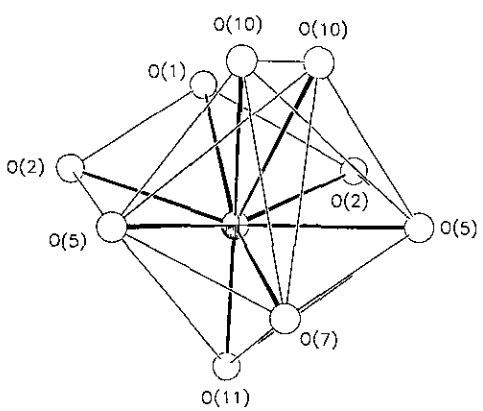


FIG. 5. ORTEP view of the K(22) coordination environment in $K_3Nb_5GeO_{16} \cdot 2H_2O$, with K represented by a shaded sphere, and O atoms by spheres of arbitrary radius. Nonbonding O · · · O contacts < 3.8 Å are represented by thin lines.

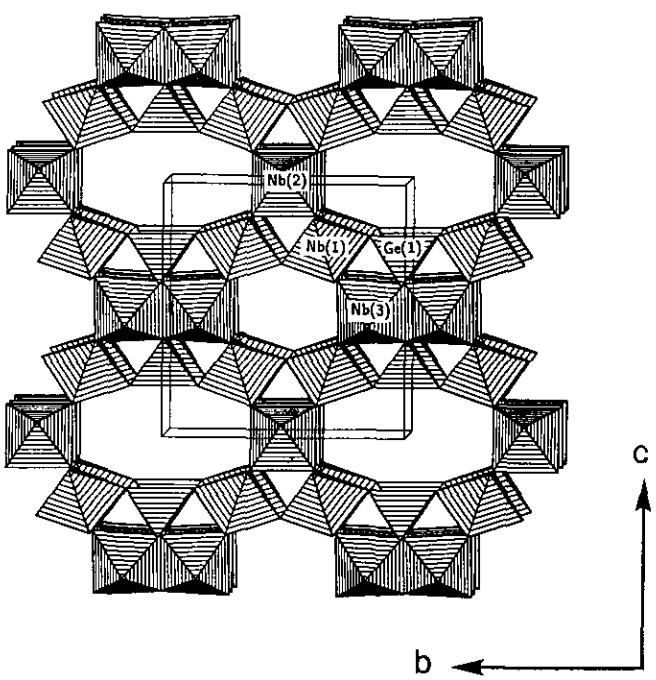


FIG. 7. Polyhedral view, just oblique to the [100] direction, of the Nb/Ge/O framework in $K_3Nb_5GeO_{16} \cdot 2H_2O$, showing the distinct 8- and 6-ring one-dimensional channels.

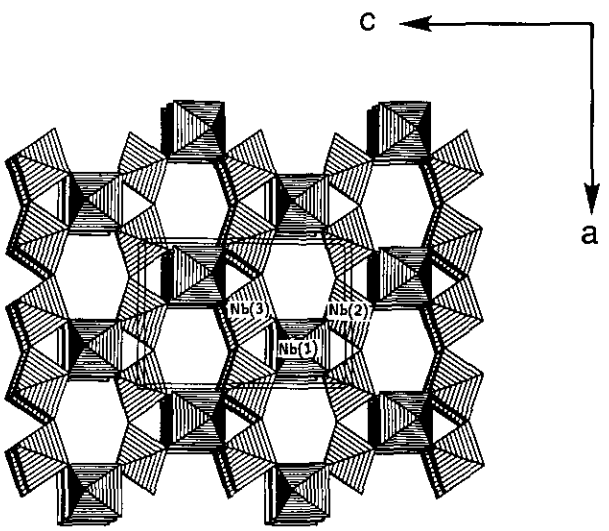


FIG. 8. Polyhedral view down [010] of the Nb/Ge/O framework in $K_3Nb_5GeO_{16} \cdot 2H_2O$, showing the one-dimensional 6-ring channels.

cules bond to the guest $K^+$ species as noted in Table 3. O(10) occupies the 6-ring [100] channel, whereas O(11) is located in the large, 8-ring [100] aperture.

The assignment of the extra-framework electron density to partially occupied K or O sites presented here is geometrically reasonable, and ensures that charge balancing is achieved, by idealizing the refined stoichiometry noted above to $K_3Nb_5GeO_{16} \cdot 2H_2O$. This analysis assumes that no "mixing" of K and O (water molecule) occurs on the same crystallographic site, although the crystal radii of $K^+$ and $H_2O$ are quite similar.

The polyhedral connectivity in $K_3Nb_5GeO_{16} \cdot 2H_2O$ leads to an open structure containing a two-dimensional channel system, as illustrated in Figs. 7 and 8 with STRUPLO-84 (22). Two types of channel are formed in the [100] direction: a "6-ring" centered at $(\frac{1}{2}, \frac{1}{2}, 0)$ and a large, squashed "8-ring" centered at (0, 0, 0). Both of these channels contain both potassium ions and water molecules, as noted above. In the [010] direction, regular "6-ring" channels occur at $(0, \frac{1}{4}, \frac{1}{4})$, which cross-connect with the [100] channels, to form a two-dimensional system. The "double channel" [100] projection of the $K_3Nb_5GeO_{16} \cdot 2H_2O$ structure is rather similar to the [001] projection of the structure of $KNb_4AsO_{13}$ (23), but the polyhedral connectivities in the other two directions in these two structures are different.

## CONCLUSIONS

$K_3Nb_5GeO_{16} \cdot 2H_2O$, a new hydrated potassium niobium germanate, has been prepared by high-pressure hydrothermal methods. It is the first well-characterized *M*/Nb/Ge/O/$H_2O$ phase, and shows another distinct structure, compared to the *M*/Nb/Ge/O phases noted in the introduction. Nb–(O,O′)–Nb edge links and Nb–O–Nb and Nb–O–Ge vertex links provide the inter-polyhedral links in $K_3Nb_5GeO_{16} \cdot 2H_2O$. We are now carrying out further exploratory syntheses in this phase space: If noncentrosymmetric phases can be prepared, they may have interesting nonlinear optical properties (24).

## ACKNOWLEDGMENT

We thank the National Science Foundation for partial financial support.

## REFERENCES

1. J. Choisnet, A. Deschanvres, and B. Raveau, *J. Solid State Chem.* **4,** 209 (1972).
2. J. Choisnet, M. Hervieu, D. Groult, and B. Raveau, *Mater. Res. Bull.* **12,** 621 (1977).
3. J. Choisnet, N. Nguyen, and B. Raveau, *Rev. Chim. Miner.* **14,** 311 (1977).
4. B. V. Mill', E. L. Belokoneva, and A. V. Butashkin, *Kristallografiya* **35,** 316 (1990).
5. J. B. Higgins and P. H. Ribbe, *Am. Mineral.* **61,** 878 (1976).
6. A. A. Kaminskii, B. V. Mill', E. L. Belokoneva, and A. V. Butashkin, *Izv. Akad. Nauk SSSR Neorg. Mater.* **27,** 1899 (1991).
7. R. J. Cava, D. W. Murphy, and S. M. Zahurak, *J. Electrochem. Soc.* **130,** 2345 (1983).
8. J. P. Giroult, M. Goreaud, P. Labbe, and B. Raveau, *J. Solid State Chem.* **44,** 407 (1982).
9. B. Domenges, M. Goreaud, P. Labbe, and B. Raveau, *J. Solid State Chem.* **50,** 173 (1983).
10. A. Leclaire, M. M. Borel, A. Grandin, and B. Raveau, *Acta Crystallogr. Sect. C* **46,** 2009 (1990).
11. C. Gueho, M. M. Borel, A. Grandin, A. Leclaire, and B. Raveau, *Z. Anorg. Allg. Chem.* **615,** 104 (1992).
12. J. P. Dougherty and S. K. Kurtz, *J. Appl. Crystallogr.* **9,** 145 (1976).
13. M. S. Lehmann and F. K. Larsen, *Acta Crystallogr. Sect. A* **30,** 580 (1974).
14. G. M. Sheldrick, "SHELXS-86 User Guide." Crystallography Department, University of Göttingen, Germany, 1986.
15. N. Walker and D. Stuart, *Acta Crystallogr. Sect. A* **39,** 158 (1983).
16. J. R. Carruthers and D. J. Watkin, *Acta Crystallogr. Sect. A* **35,** 698 (1979).
17. A. C. Larson, *Acta Crystallogr.* **23,** 664 (1967).
18. "*International Tables for X-Ray Crystallography*," Vol. IV. Kynoch Press, Birmingham 1974.
19. D. J. Watkin, J. R. Carruthers, and P. W. Betteridge, "CRYSTALS User Guide," Chemical Crystallography Laboratory, Oxford University, United Kindom, 1985.
20. R. D. Shannon, *Acta Crystallogr. Sect. A* **32,** 751 (1976).
21. N. E. Brese and M. O'Keefe, *Acta Crystallogr. Sect. B* **47,** 192 (1991).
22. R. X. Fischer, *J. Appl. Crystallogr.* **18,** 258 (1985).
23. A. Heddard, T. Jouini, Y. Piffard, and N. Jouini, *J. Solid State Chem.* **77,** 293 (1988).
24. C. S. Liang, W. T. A. Harrison, M. M. Eddy, T. E. Gier, and G. D. Stucky, *Chem. Mater.* **5,** 917 (1993).